Paper No. 226

ISMS 2016

Large scale panel destress blasting parametric study

Isaac Vennes*, Hani Mitri

Department of Mining and Materials Engineering, McGill University, Montreal, Canada, H3A 0E8

ABSTRACT

The purpose of this parametric study is to quantify the effect of panel destressing on a steeply dipping remnant ore pillar. A large-scale destress blast program is simulated in the hanging wall of the ore pillar using the finite difference program FLAC3D. The simplified model consists of a 10MT ore pillar divided into 20 stopes on two levels. Two panels are destressed in the hanging wall to cover 8 stopes, followed by the mining of 4 stopes in the stress shadow in a retreat sequence. The varied parameters are the rock fragmentation factor (α) and stress reduction factor (β) of the destress panel. The effect of panel destressing is evaluated based on the volume of ore at risk in the stress shadow as well as the sudden stress change in the stope caused by the destress blast. Overall, a successful blast with a realistic stress reduction factor and rock fragmentation factor reduces the major principal stress in the nearest stopes by 10 MPa to 25 MPa. This yields a reduction of ore at risk volume ranging from 8% to 50% in the stress shadow as the first 4 stopes are mined.

1. INTRODUCTION

Rockbursts occur when the rock has been loaded beyond its failure point, manifesting as a sudden and violent failure of rock. Contributing factors to the occurrence of rockbursts are high stress, stiff strata, rapid mining rate, and large excavation area among others.

Destress blasting is a rockburst control technique which employs explosives to fracture the rock, reducing its stiffness and releasing stored elastic strain energy. To reduce the risk of rockbursts, destress blasting can be directly applied to the rock to be extracted such as for drift development and crown pillar destressing for overhand cut and fill. Another strategy is panel destressing, where relatively large volumes of rock (greater than 10 Kt) are destressed in the hanging wall of the orebody, such that the ore to be bulk mined lies in the stress shadow of the destress panel. In this case, panel destress blasting aims to reduce the risk of rockbursts by reducing the magnitude of the major principal stress in the ore to be mined. This strategy has been applied Star Morning Mine (Karwoski and McLaughin 1975), in Brunswick mine (Andrieux 2005; Andrieux, et al. 2000) and Fraser mine (Andrieux 2005). The two latter applications were deemed successful based on recorded stress changes, seismicity, and measured displacements. At Fraser Mine, a sudden decrease of 1.5 MPa in the direction major principle stress was recorded in the stress shadow 25 meters away from panel. In Brunswick mine, a sudden 4 MPa stress drop in the direction of the major principal stress was measured 20 meters away from panel.

In both case studies, the magnitude of the sudden and long term stress decrease in the stress shadow appears to be a small proportion of the mining induced major principal stress. To evaluate the effectiveness of the panel destress blasting strategy, the effect of this stress decrease on the burst proneness of the ore in the pillar needs to be examined. In this paper, a parametric study is conducted with a linear elastic numerical model. The purpose is to quantify effect of destress blasting in terms of stress reduction and ore at risk in the panel stress shadow by varying the rock fragmentation factor (α) and the stress reduction factor (β).

2. DESTRESS BLASTING MECHANISMS

Destress blasting is understood to reduce the stress borne in rock by inducing fracturation, demonstrated to be along pre-existing fracture planes (Lightfoot et al., 1996). This induced fracturation is thought to have multiple effects that reduce burst proneness. Firstly, the induced fracturation reduces the stiffness of the rock (Blake, 1972) as well as the load bearing ability. Secondly, as the blast induced cracks propagate, the stored elastic strain energy is dissipated as seismic energy (Tang and Mitri, 2001), resulting in an instantaneous reduction of stresses in the rock. Finally, destress blasting mobilizes the rock mass along pre-existing fractures, equivalent to plastic strain. As rockbursts are normally associated to brittle elastic rock failure, a destressed zone will yield gradually rather than fail suddenly as a rockburst (Saharan, 2004). However, when examining the effectiveness of panel destressing with a linear elastic model, the modification of the failure mechanism in the panel will not affect the burst potential of the destressed ore. Therefore, only the

*Isaac Vennes – email : isaac.vennes@mail.mcgill.ca

former two effects need to be considered in this study.

3. DESTRESS BLASTING MODEL

3.1 Modelling Technique

Multiple techniques have been developed to simulate destress blasting, starting with the rock fragmentation factor α (Blake, 1972), which reduces the Young's modulus of the rock targeted by the destress blast. Tang (2000) expanded on Blake's fragmentation factor by adding the stress reduction factor to take into account the strain energy that is instantaneously released by the blast as seismic energy. Tang deems the inclusion of β necessary in light of case studies where α is unrealistically low; a realistic range for α is 0.4 – 0.6, combined with β>0.4. Finally, Saharan (2005) proposed that α and β should vary anisotropically, since blast induced fractures tend to propagate in the direction of the major principal stress.

In this study, the technique described by Tang (2000) is applied to the destress panels. Six combinations of α and β are tested, assumed to lie along the line α+β=1. The most optimistic combination with highest rock fragmentation and stress reduction tested is α=0 and β=1, equivalent to the panel material being extracted. The combination with lowest stress reduction and rock fragmentation tested is α=0.8 and β=0.2. A base case model with no destress blast is also run (α=1, β=0). The parameters α and β are assumed isotropic.

To simulate a destress panel, the modulus of elasticity is reduced in the panel by the factor α which ranges from 0 to 1:

$$E_{destress} = E\alpha \quad [1]$$

In addition, the residual stress tensor in the targeted zones is applied following the equation:

$$\{\sigma_D\} = (1 - \beta) \cdot \{\sigma\} \quad [2]$$

where β ranges from 0 to 1, and where

$$\{\sigma\}^T = \left(\sigma_{xx}, \sigma_{yy}, \sigma_{zz}, \sigma_{xy}, \sigma_{yz}, \sigma_{xz}\right) \quad [3]$$

The balanced stress state in the panel prior to destressing is replaced with the residual stress state $\{\sigma_D\}$ defined by equation [3]. This removes a proportion of the strain energy in the panel equal to the factor β, causing an imbalance between the model boundary work and strain energy in model. A new equilibrium reached after solving model where the final stress tensor in the panel lies between the initial stress tensor and the residual stress tensor.

3.2 Panel Geometry

The total mass targeted by a destress blast can be estimated based on the drill hole diameter (Andrieux, 2005). Assuming 2 rows of blastholes, the targeted mass M_e can be estimated as:

$$M_e = 2 * (16 * d) * H * L * \rho_r \quad [4]$$

where d is the blasthole diameter, H the height of the panel, L the strike length of the panel, and ρ_r the density of the rock. The explosive energy applied in reported destress blasting case studies ranges from 10 cal/kg to 500 cal/kg (Andrieux, 2005). Since most applications of destress blasting aim to directly pre-condition the rock to be extracted, the applied explosive energy is low and the drill hole diameter small: 43 mm to 54 mm for Creighton Mine (O'Donnell, 1992; Oliver et al., 1987), 45 mm for Campbell Mine (Makuch et al., 1987), and 35 mm to 63.5 mm for Macassa Mine (Hanson et al., 1987).

However, panel destressing case studies all lie on the high end of this range (200-500 cal/kg) with large blasthole diameters ranging from 115 mm for Star Morning mine (Karwoski and McLaughin, 1975) and Fraser Mine (Andrieux, 2005) to 165 mm for Brunswick Mine (Andrieux et al., 2000). Based on equation 4, the targeted panel thickness based on the reported blasthole diameters ranges from 3.7 m to 5.3 m. In this study, a 3 m panel thickness is assumed, equivalent to two rows of 3.5″ (89 mm) blastholes.

4. EVALUATION OF STRAINBURST POTENTIAL

The first step of the study is to confirm need for destress blasting. For a linear elastic numerical model, the available criteria are either based on energy or stress state. Multiple methods based on energy calculations have been proposed such as the Energy Release Rate (ERR) (Cook, 1967), and the Burst Potential Index (BPI) (Mitri et al., 1999). However, a limitation of ERR is that rock mass critical strain energy is not factored in. The ERR is therefore not a suitable criterion for this study, as it does not evaluate the need for destressing, only its effect. On the other hand, the BPI defined by Mitri is for uni-axial conditions and therefore only applicable to stope and drift faces and not to bulk of pillar.

Finally, the brittle shear ratio (BSR) was developed based on a study by Martin and Kaiser (1999), where rock was found to undergo brittle shear as the ratio between the deviatoric stress and the uni-axial compressive strength exceeded 0.4. The BSR proposed by Castro et al. (1997), is expressed as:

$$BSR = \frac{\sigma_1 - \sigma_3}{UCS_{intact}} \quad [5]$$

The risk of strainbursts was deemed significant when the ratio exceeds 0.7. Therefore, ore zones with a BSR exceeding 0.7 are termed 'at risk'. With an initial pillar BSR due to mining induced stresses at 0.2, there is no immediate need to destress. However, after the extraction of first 4 stopes, 11.4% of the remaining ore is at risk, equivalent to 36000 tonnes.

5. MODEL CONSTRUCTION

5.1 Model Geometry

Pillar and panel zones are built manually with finite difference numerical modelling software FLAC3D. Host rock zones and ore zones that are not in pillar generated with Kubrix (Itasca, 2016). The pillar hanging wall and footwall are vertical. The pillar consists of 20 stopes on 2 levels, with 10 stopes per level. On each level, there are 5 stopes along the orebody strike, 2 along the thickness. The stope dimensions are 12 m x 15 m x 30 m (strike x thickness x height). The panel dimensions are 15 m x 3 m x 60 m (strike x thickness x height).

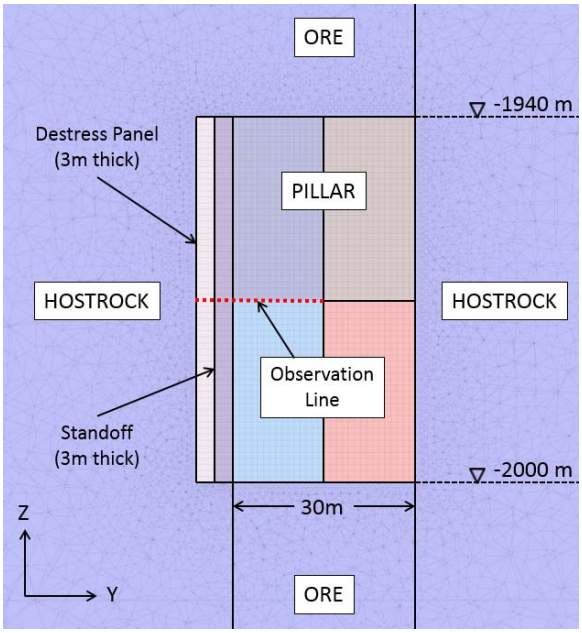

Figure 1: Model elevation view along orebody thickness. Strike of the orebody and pillar is 60 m in the x-direction.

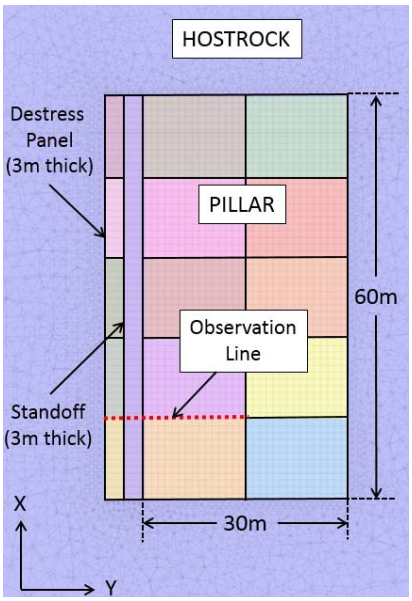

Figure 2: Model plan section view of the ore pillar.

The model boundary is set 160 meters away from the pillar, such that the pillar extraction causes a stress change smaller than 1% at the boundary. For the mesh sensitivity analysis, the zone size in the pillar is kept constant at 1 m x 1 m x 1 m, while the boundary surface mesh is varied from 8 m x 8 m to 15 m x 15 m. Monotonic convergence of maximum displacement is obtained at 10 m x 10 m boundary mesh (see Figure 1). This yields an optimal model with 1500000 elements. The panel zones are 0.25 meters along the panel thickness, 1 m along the panel strike, and 1 m along the panel height.

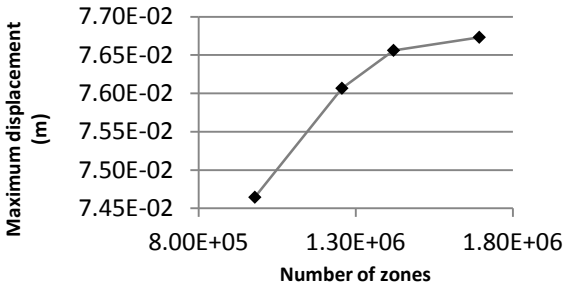

Figure 3: Model mesh sensitivity analysis.

5.2 Model Material Properties

Table 1: Material properties.

	Young's Modulus (GPa)	Poisson's Ratio	Unit Weight (MN/m^3)	Intact UCS (MPa)
Ore	27.6	0.28	0.037	140
Host Rock	37.8	0.24	0.029	150
Backfill	2.0	0.30	0.024	N/A

The numerical model is linear elastic. The elastic material properties are shown in Table 1, along with the intact UCS. The properties are provided by a case study mine.

5.3 Model Loading

The model external x-face constrained in the x direction, the model external y-face constrained in y direction. Bottom face constrained in z-direction. The top boundary free, with applied overburden stress.

$$\sigma_3\ (MPa) = \sigma_{zz} = 0.029 * depth\ (m) \quad [6]$$

The far field x and y stress are initialized in all zones following equations [7] and [8], adjusting for the effect of Poisson's ratio due to model weight. The initial stresses are oriented such that the major principal stress is perpendicular to the orebody and panel strike.

$$\sigma_1(MPa) = \sigma_{yy} = 10.825 + 0.032 * depth\ (m) \quad [7]$$

$$\sigma_2(MPa) = \sigma_{xx} = 8.687 + 0.024 * depth\ (m) \quad [8]$$

5.4 Mining Sequence

To set up the ore pillar, the orebody is mined bottom up in 10 stages, with vertical lifts ranging from 30 to 40 meters. The ore above the pillar is mined first. After each lift, the void is backfilled. Each stope is mined in six 5 meter lifts. The pillar is mined in retreat from hanging wall to footwall, west to east, bottom to top. For the parametric study, 2 panels are destressed simultaneously and the first 4 stopes of the described sequence are mined in the stress shadow.

6. RESULTS

The effect of panel destressing is quantified in terms of the stress drop over the strike of the hanging stopes and in terms of ore at risk (BSR>0.7) in the stress shadow of the panel. To begin, the major principal stress in the pillar is 80 MPa following extraction of upper and lower orebody. The variation of major principal stress in the stress shadow for varying destress blasting input parameters is shown in Figure 3. The stress drop in proportion to the initial stress in the stope is shown in Figure 4.

For a high rock fragmentation and stress reduction effect (α=0.1, β=0.9), an immediate stress drop of 10 MPa to 25 MPa is obtained in the hanging wall stope (10% to 30% stress change). Immediately after the destress blast, the volume of ore at risk in the stress shadow is reduced by 10%. After extracting 4 stopes in the stress shadow, the destress blast reduces the volume of ore at risk by 50% as shown in Figure 5. On the other hand, for a low rock fragmentation and stress reduction effect (α=0.8, β=0.2), the obtained stress reduction is below 3 MPa (4% stress change). The destress blast yields an immediate 2% reduction of ore at risk. After 4 stopes, the destress blast reduces ore at risk by 5%.

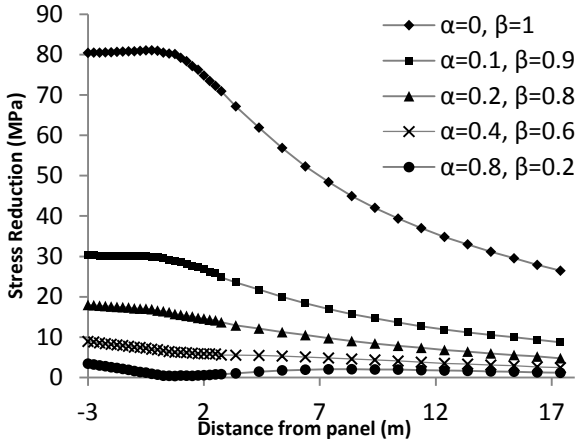

Figure 4: σ_{yy} drop due to destress blast along observation line shown in Figures 1 and 2.

In both cases, the destressing effect is not detectable immediately after the destress blast with the ore at risk criterion. Since the bulk of the pillar BSR is well below 0.7, the destress blasting stress reduction in shadow does not necessarily translate to reduction of ore at risk. Comparison with the destress blasting case studies of Brunswick mine and Fraser Mine, where a 4 MPa drop at 20 meters and a 1.5 MPa drop 25 meters were measured in the direction of the major principal stress immediately after the destress blast, suggests that 0.2<α<0.4 and 0.6<β<0.8. Applying these destress blasting parameters to the parametric study model yields a reduction of ore at risk ranging from 8% to 50% in the stress shadow during the extraction of the first 4 stopes.

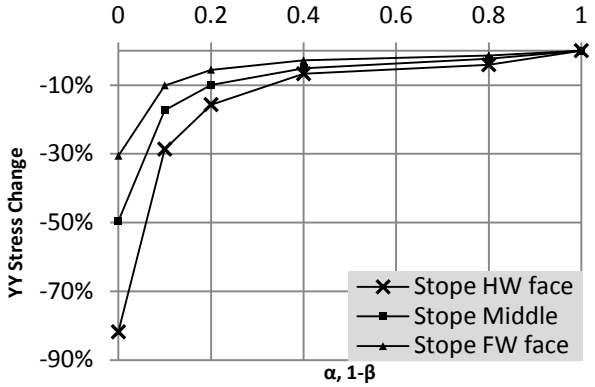

Figure 5: σ_{yy} change in HW stope. Observation points are along the observation line shown in Figures 1 and 2.

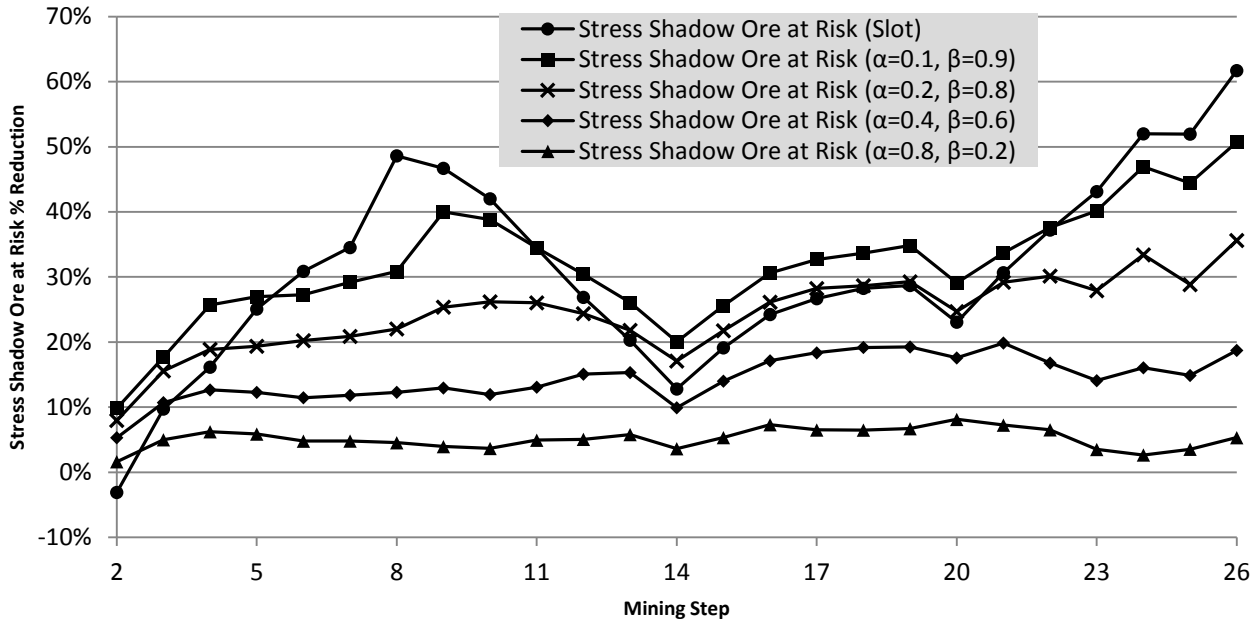

Figure 6: Ore at risk reduction in stress shadow with respect to scenario with no destress blast. Shown are the destress blast (step 2), extraction of stope 1 (steps 3-8), extraction of stope 2 (9-14), extraction of stope 3 (15-20), extraction of stope 4 (21-26).

7. CONCLUSIONS

In this study, panel destress blasting is shown to reduce the volume of ore at risk in a highly stressed ore pillar by 8% to 50% in the stress shadow, given an obtained rock fragmentation factor between below 0.4 and a stress reduction factor above 0.6. These values are realistic when compared to the observed immediate stress changes at Brunswick Mine and Fraser Mine following a panel destress blast, where 200-500 kcal/kg of explosive energy was applied. Panel destressing can therefore be an effective tool to reduce risk to operations when bulk mining the ore pillar.

However, it is assumed in the parametric study that the pre-mining major principal stress is normal to the destress panel. Also, the destressed modulus of elasticity and stress release are assumed to be isotropic. These results therefore reflect a best case scenario for a panel destressing program.

8. REFERENCES

Andrieux P (2005) Application of rock engineering systems to large-scale confined destress blasts in underground pillars. Laval University

Andrieux P, Brummer R, Liu Q, Mortazavi A, Simser B (2000) Large-Scale Panel Destress Blast at Brunswick Mine. In: 23rd Study Dession on Blasting Techniques, vol. SEEQ, Quebec

Blake W (1972) Rock-burst mechanics. Quarterly of the Colorado School of Mines 67(1):1-64

Castro LAM, Grabinsky MW, McCreath DR (1997) Damage inititiation through extension fracturing in a moderately jointed brittle shear rock mass. International Journal of Rock Mechanics and Mining Sciences (34):110-113

Cook NGW (1967) Design of underground excavations. In: 8th US Rock Mechanics Symposium, Minnesota, pp 167-193

Hanson D, Quesnel W, Hong R (1987) Destressing a Rockburst Prone Crown Pillar: Macassa Mine. In, CANMET

Itasca (2016), Kubrix [Computer Software]; retrieved from www.itascacg.com/software/kubrix

Karwoski WJ, McLaughin WC (1975) Rock pre-conditioning to prevent rockbursts - report on a field demonstration. In, vol. United States Department of the Interior, Bureau of Mines

Lightfoot N, Kullman DH, Toper AZ, Stewart RD, Gronder M, Rensburg ALJv, Longmore PJ (1996) Preconditioning to Reduce the Incidence of Face Bursts of Highly Stressed Faces. In, vol. CSIR: MININGTEK

Makuch A, Neumann M, Hedley DGF, Blake W (1987) Destress Blasting at Campbell Red Lake Mine. In: Canada/Ontario/industry Rockburst Research Project, CANMET, Elliot Lake Laboratory

Martin CD, Kaiser PK (1999) Predicting the depth of stress induced failure around underground excavations in brittle rocks. In: 49th Canadian Geothechnical Conference, St-John's, pp 105-114

Mitri HS, Tang B, Simon R (1999) FE modelling of mining-induced energy release and storage rates.

The Journal of the South African Insitute of Mining and Metallurgy:103-110

O'Donnell JDP (1992) The use of destress blasting at Inco's Creighton Mine. In: MASSMIN 92, vol. SAIMM, Johannesburg, pp 71-74

Oliver P, Wiles T, MacDonald P, O'Donnel D (1987) Rockburst control measures at Inco's Creighton Mine. In: 6th Conference on Ground Control in Mining, West Virginia

Saharan MR (2004) Dynamic Modelling of Rock Fracturing by Destress Blasting. McGill University

Tang B (2000) Rockburst Control using Destress Blasting. McGill University

Tang B, Mitri HS (2001) Numerical modelling of rock preconditioning by destress blasting. Ground Improvement 5:1-11